OPEN ACCESS
CellPress

Cell Reports
Report

Activation of Neuronal Gene Expression by the JMJD3 Demethylase Is Required for Postnatal and Adult Brain Neurogenesis

Dae Hwi Park,[1,2,3] Sung Jun Hong,[1,2] Ryan D. Salinas,[1,2] Siyuan John Liu,[1,2] Shawn W. Sun,[1,2,3] Jacopo Sgualdino,[4] Giuseppe Testa,[4] Martin M. Matzuk,[5,6,7,8,9,10] Naoki Iwamori,[5,9,11] and Daniel A. Lim[1,2,3,*]

[1]Department of Neurological Surgery, University of California, San Francisco, San Francisco, CA 94143, USA
[2]Eli and Edythe Broad Center of Regeneration Medicine and Stem Cell Research, University of California, San Francisco, San Francisco, CA 94143, USA
[3]Veterans Affairs Medical Center, University of California, San Francisco, San Francisco, CA 94143, USA
[4]European Institute of Oncology (IEO), IFOM-IEO Campus, Via Adamello 16, 20139 Milan, Italy
[5]Department of Pathology and Immunology, Baylor College of Medicine, Houston, TX 77030, USA
[6]Department of Molecular and Cellular Biology, Baylor College of Medicine, Houston, TX 77030, USA
[7]Department of Molecular Human Genetics, Baylor College of Medicine, Houston, TX 77030, USA
[8]Department of Pharmacology, Baylor College of Medicine, Houston, TX 77030, USA
[9]Center for Reproductive Medicine, Baylor College of Medicine, Houston, TX 77030, USA
[10]Center for Drug Discovery, Baylor College of Medicine, Houston, TX 77030, USA
[11]Center of Biomedical Research, Research Center for Human Disease Modeling, Graduate School of Medical Sciences, Kyushu University, Fukuoka 812-8582, Japan
*Correspondence: limd@neurosurg.ucsf.edu
http://dx.doi.org/10.1016/j.celrep.2014.07.060

SUMMARY

The epigenetic mechanisms that enable lifelong neurogenesis from neural stem cells (NSCs) in the adult mammalian brain are poorly understood. Here, we show that JMJD3, a histone H3 lysine 27 (H3K27) demethylase, acts as a critical activator of neurogenesis from adult subventricular zone (SVZ) NSCs. JMJD3 is upregulated in neuroblasts, and *Jmjd3* deletion targeted to SVZ NSCs in both developing and adult mice impairs neuronal differentiation. JMJD3 regulates neurogenic gene expression via interaction at not only promoter regions but also neurogenic enhancer elements. JMJD3 localizes at neural enhancers genome-wide in embryonic brain, and in SVZ NSCs, JMJD3 regulates the I12b enhancer of *Dlx2*. In *Jmjd3*-deleted SVZ cells, I12b remains enriched with H3K27me3 and *Dlx2*-dependent neurogenesis fails. These findings support a model in which JMJD3 and the poised state of key transcriptional regulatory elements comprise an epigenetic mechanism that enables the activation of neurogenic gene expression in adult NSCs throughout life.

INTRODUCTION

Epigenetic regulation via histone methylation is critical for the establishment and maintenance of lineage-specific gene expression. The trimethylation of histone 3 at lysine 27 (H3K27me3) by Polycomb repressive complex 2 (PRC2) correlates with transcriptional repression (Margueron and Reinberg, 2011), and such gene repression is critical for the proper function of stem cells in both the embryonic and adult brain (Hirabayashi and Gotoh, 2010). While previous studies have highlighted the importance of H3K27me3 placement and gene repression in neural development (Hirabayashi et al., 2009; Hwang et al., 2014; Pereira et al., 2010), how H3K27me3 is removed for the activation of neurogenic gene expression is not well understood.

JMJD3 (KDM6B) is an H3K27me3-specific demethylase that belongs to the family of JmjC domain-containing proteins (Agger et al., 2007; De Santa et al., 2007). *Jmjd3* null mice die at birth due to respiratory failure (Burgold et al., 2012; Satoh et al., 2010). In the embryonic mouse forebrain, *Jmjd3* expression is regulated (Jepsen et al., 2007), and in embryonic stem cells (ESCs), JMJD3 is required for neural commitment (Burgold et al., 2008). While knockdown studies in the embryonic spinal cord and retina indicate developmental roles for *Jmjd3* (Akizu et al., 2010; Iida et al., 2014), the function of JMJD3 in adult neural stem cells (NSCs) has not been reported.

The adult mammalian brain harbors NSCs in the subventricular zone (SVZ) and dentate gyrus of the hippocampus (Fuentealba et al., 2012; Ming and Song, 2011). The epigenetic mechanisms required to maintain lifelong neurogenesis in these germinal zones are only beginning to be elucidated (Gonzales-Roybal and Lim, 2013; Ma et al., 2010). Emerging evidence indicates that dynamic changes of chromatin modifications at transcriptional enhancers are a strong determinant of gene expression (Calo and Wysocka, 2013). Like promoters, the activity of enhancers can be "poised" by the presence of repressive H3K27me3 (Rada-Iglesias et al., 2011), suggesting that transcription can be activated by the action of H3K27me3-specific

demethylases at enhancer regions. Our data support a model in which adult NSCs maintain a distinct set of transcriptional regulatory elements in a poised chromatin state, and that JMJD3 can rapidly activate lineage-specific gene expression via H3K27 demethylation at specific genomic regions including enhancers.

RESULTS

JMJD3 Is Expressed in the Adult SVZ Neurogenic Lineage

Throughout adult life, SVZ NSCs (type B1 cells) produce transit-amplifying cells (type C cells), which give rise to neuroblasts (type A cells) that migrate to the olfactory bulb (OB), where they become interneurons (Figures S1A and S1B). RNA sequencing (RNA-seq) and in situ hybridization analysis revealed prominent *Jmjd3* expression in the SVZ, the neuroblast rostral migratory stream (RMS), and OB (Figures S1C and S1D) (Lein et al., 2007). SVZ NSCs express glial fibrillary acidic protein (GFAP), and many (79.5%, n = 30/38) GFAP+ SVZ cells exhibited nuclear JMJD3 (Figure S1E). Transit-amplifying cells and neuroblasts express DLX2, and most (97.6%, n = 280/287) DLX2+ cells coexpressed JMJD3 (Figures S1F and S1I). JMJD3 was also present in doublecortin (DCX)+ neuroblasts (Figure S1G). Thus, JMJD3 is expressed SVZ NSCs as well as their neurogenic daughter cells.

JMJD3 Is Required for Postnatal OB Neurogenesis

To study the role of JMJD3 in SVZ-OB neurogenesis, we used a conditional knockout allele of *Jmjd3* (*Jmjd3*$^{F/F}$, Figures S2A–S2C). Mice with the *hGFAP-Cre* transgene exhibit excision of conditional alleles in SVZ NSC precursors at embryonic day 13.5 (E13.5) (Lim et al., 2009), and SVZ cells of *hGFAP-Cre;Jmjd3*$^{F/F}$ mice were JMJD3 negative (Figure S1J). *hGFAP-Cre;Jmjd3*$^{F/F}$ mice and their littermate controls (wild-type and *hGFAP-Cre;Jmjd3*$^{F/+}$) were born at the expected Mendelian ratios and were similar in size, weight, and overall survival.

To assess OB neurogenesis, we injected postnatal day 30 (P30) mice with 5-bromo-2-deoxyuridine (BrdU) to label a cohort of newly born SVZ neuroblasts and analyzed the OB for BrdU+ neurons 10 days later. In the *hGFAP-Cre;Jmjd3*$^{F/F}$ OBs, there were approximately 50% fewer BrdU+, NeuN+ neurons (Figures 1A–1C), which was not likely related to changes in neuronal survival, as the number of activated caspase-3+ OB cells was not increased (Figure 1D).

To evaluate the production of neuroblasts in the SVZ, we administered the thymidine analog ethynyl deoxyuridine (EdU) to mice 1 hr before being culled. In P40 *hGFAP-Cre;Jmjd3*$^{F/F}$ mice, there were 2- to 3-fold fewer DCX+, EdU+ cells in the SVZ (Figures 1H–1I). Furthermore, the expression of DLX2, a key neurogenic transcription factor, was strongly reduced (Figures 1K and 1K′). Despite there being fewer EdU+ cells in *hGFAP-Cre;Jmjd3*$^{F/F}$ mice, the dorsal SVZ was abnormally expanded with DCX+ cells (Figures 1F–1G′ and S2D–S2F′). Defective neuroblast migration can result in the postnatal accumulation of DCX+ cells in the SVZ (Lim et al., 2009); in *hGFAP-Cre;Jmjd3*$^{F/F}$ mice, the neuroblast migratory pathways were highly disorganized (Figures S2K and S2K′), and many SVZ cells pulse-labeled with BrdU failed to migrate from the SVZ (Figures S2G–S2I′). Thus, in *hGFAP-Cre;Jmjd3*$^{F/F}$ mice, the addition of new neurons to the OB was abrogated by a decrease in SVZ neurogenesis as well as abnormal neuroblast migration.

Adult SVZ NSCs (type B1 cells) contact the ventricle with a specialized apical surface located at the center of a pinwheel-like structure composed of ependymal cells (Mirzadeh et al., 2008). Interestingly, adult *hGFAP-Cre;Jmjd3*$^{F/F}$ mice had 3- to 4-fold more SVZ cells with such ventricular contact (Figures S2M–S2O). As is characteristic of type B1 cells, these apical surfaces had solitary basal bodies and were GFAP+ (Figures S2P–S2S′). This accumulation of type B1-like cells was evident by P7 (Figures S3A–S3L′) and not likely related to cell proliferation (Figures S3M–S3R′). Thus, although *hGFAP-Cre;Jmjd3*$^{F/F}$ mice had greater numbers of cells with SVZ NSC characteristics, the production of neuroblasts was reduced, suggesting that the ventricle-contacting SVZ cells in *hGFAP-Cre;Jmjd3*$^{F/F}$ mice are defective for neurogenesis.

Jmjd3 Deletion Targeted to Adult SVZ NSCs Inhibits OB Neurogenesis

To test whether *Jmjd3* plays a role in adult neurogenesis independent of its potential function in postnatal SVZ NSC development, we targeted *Jmjd3*-deletion to SVZ NSCs in adult mice (Figures 1L–1M′). Stereotactic injection of the Ad:GFAP-Cre adenovirus into the SVZ induces Cre-mediated recombination in GFAP+ NSCs (Mirzadeh et al., 2008). We injected Ad:GFAP-Cre into the SVZ of P60-90 *Jmjd3*$^{F/F}$ mice or littermate controls (*Jmjd3*$^{F/+}$) that carry the Ai14-tdTomato Cre-reporter transgene. To control for experimental variation related to the stereotactic injection itself, the Ad:GFAP-Cre adenovirus was mixed and coinjected with a lentivirus that constitutively expresses only GFP (lenti-GFP).

We quantified the number of tdTomato+ OB neurons in *Jmjd3*$^{F/F}$;Ai14 and control;Ai14 mice 14 days after injection (Figures 1N–1P). For each mouse, the number of tdTomato+ OB neurons was normalized to the number of GFP+ OB neurons. In control;Ai14 mice, there were 5.5 tdTomato+ cells per 10 GFP+ cells in the OB. In contrast, there were only 2.0 tdTomato+ cells per 10 GFP+ cells in the OB of *Jmjd3*$^{F/F}$;Ai14 mice. Thus, *Jmjd3*-deleted SVZ NSCs produced 60% fewer OB neurons than NSCs in control mice. Furthermore, in the SVZ of *Jmjd3*$^{F/F}$ mice, there were 24% fewer DLX2+, tdTomato+ cells (Figures S2T–S2W). Taken together, these results indicate that adult NSCs require *Jmjd3* for SVZ-OB neurogenesis.

Jmjd3 Regulates the Differentiation of SVZ NSCs

We next used SVZ NSCs monolayer cultures to study JMJD3 function. During differentiation, SVZ NSCs upregulated *Jmjd3*, correlating with increased *Dlx2* expression (Figures S4A–S4G). Short-hairpin RNA (shRNA) *Jmjd3*-knockdown lentiviruses (LV-KD1-GFP and LV-KD2-GFP) strongly reduced *Jmjd3*. *Jmjd3* knockdown reduced *Dlx2* expression, but not the expression of proneural *Mash1*, PRC2 component *Ezh2*, or *Utx* (*Kdm6a*), the other known H3K27me3-specific demethylase (Figures 2A and 2B).

To target shRNA knockdown to GFAP+ SVZ NSCs, we used an EnvA-pseudotyped lentivirus and tva receptor transgenic mouse strategy (Holland et al., 1998; Lewis et al., 2001) (Figure 2A). In self-renewal conditions, *Jmjd3* knockdown in

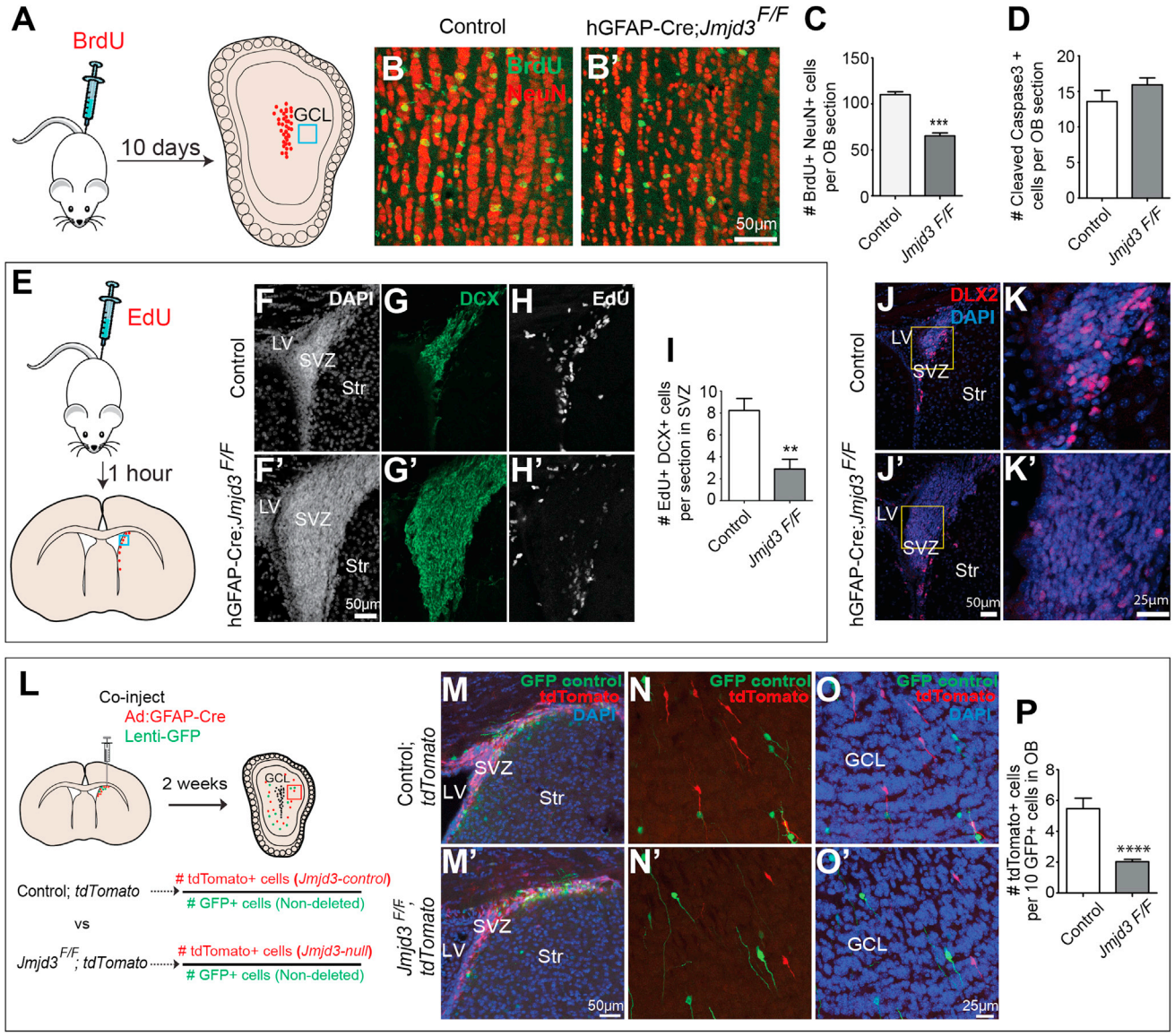

Figure 1. *Jmjd3* Is Required for Adult OB Neurogenesis

(A) Illustration of the experimental design for (B)–(D). The blue box indicates regions of shown in (B) and (B′). GCL, granule cell layer.

(B) Analysis of OB neurogenesis. Immunohistochemistry (IHC) for BrdU (green) and NeuN (red) in coronal OB sections of control (B) and *hGFAP-Cre;Jmjd3*$^{F/F}$ mice (B′).

(C) Quantification of BrdU+, NeuN+ OB neurons (***$p < 0.001$; n = 4 each; error bars represent SEM).

(D) Quantification of cleaved caspase-3+ OB cells ($p = 0.1933$; n = 4 each; error bars represent SEM)

(E) Illustration of the experimental design for (F)–(I). EdU was injected 1 hr before analysis.

(F–I) Analysis of cell proliferation and neuroblasts in the SVZ.

(F–H) DAPI+ (white), DCX+ (green), and EdU+ (white) cells in the SVZ of control mice. (F′–H′) DAPI+ (white), DCX+ (green), and EdU+ (white) cells in the SVZ of *hGFAP-Cre;Jmjd3*$^{F/F}$ mice.

(I) Quantification of EdU+, DCX+ cells in SVZ coronal sections (n = 3 each; error bars represent SEM; **$p < 0.01$).

(J–K′) Analysis of DLX2 expression in the SVZ. IHC for DLX2 (red) in SVZ coronal sections of control (J–K) and *hGFAP-Cre;Jmjd3*$^{F/F}$ mice (J′–K′). (K) and (K′) are higher-magnification views of the yellow boxed region in (J) and (J′).

(L) Schematic illustration of the experimental design for (M)–(P). Ad:GFAP-Cre virus (to delete floxed alleles in GFAP+ SVZ NSCs) and GFP lentivirus (injection control) were coinjected into the adult SVZ of *tdTomato;Jmjd3*$^{F+}$ (M–O) or *tdTomato;Jmjd3*^{FF} (M′–O′) mice.

(M–P) Analysis of OB neurogenesis. IHC for GFP (green) and tdTomato (red) in adult SVZ coronal sections of *tdTomato;Jmjd3*$^{F+}$ (M) and *tdTomato;Jmjd3*^{FF} mice (M′).

(N–O′) IHC for GFP (green) and tdTomato (red) in coronal OB sections of *tdTomato;Jmjd3*$^{F+}$ (N and O) and *tdTomato;Jmjd3*^{FF} mice (N′ and O′) 14 days after injection.

(P) Quantification of tdTomato+ neurons per ten GFP+ neurons in the OB (****$p < 0.0001$; n = 4 per group; error bars represent SEM). LV, lateral ventricle; Str, striatum; GCL, granule cell layer.

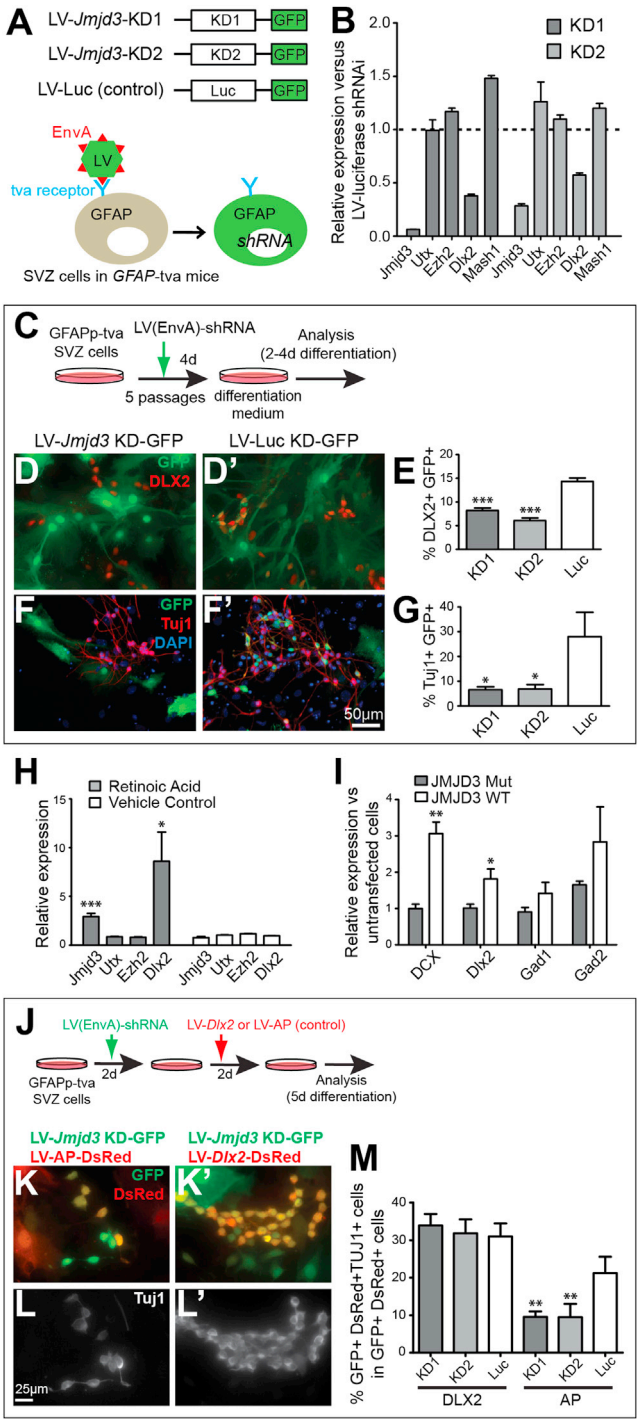

Figure 2. *Jmjd3* Regulates SVZ NSC Differentiation

(A) EnvA and *hGFAPp-tva* strategy of targeting knockdown to GFAP+ SVZ NSCs. EnvA (red) pseudotyped lentiviruses can only infect cells with the tva receptor (blue), which is expressed from the GFAP-tva transgene.

(B) Quantitative RT-PCR (qRT-PCR) analysis of LV-*Jmjd3* knockdown in SVZ NSCs (error bars represent SEM).

(C) Illustration of the experimental design for (D)–(G).

(D) ICC for GFP (green) and DLX2 (red) with LV-sh-*Jmjd3* (D) and LV-sh-luciferase (D′).

(E) Quantification of DLX2+ cells.

(F) ICC for GFP (green) and Tuj1 (red) with LV-sh-*Jmjd3* (F) and LV-sh-luciferase (F′).

(G) Quantification of Tuj1+ cells (error bars represent SEM of quadruplicate cultures; *p < 0.05, ***p < 0.001).

(H) qRT-PCR analysis of retinoic acid treatment of SVZ NSCs (***p < 0.001; *p < 0.05; n = 6 per group; error bars represent SEM).

(I) qRT-PCR analysis of *Jmjd3* overexpression in SVZ NSCs (**p < 0.01, *p < 0.05; n = 3; error bars represent SEM).

(J) Illustration of the experimental design for (K) –(M).

(K–M) Analysis of neuronal differentiation in *Jmjd3*-deficient cells after *Dlx2* overexpression.

(K–L′) IHC for Tuj1 (white) in *Jmjd3*-deficient cells with *Dlx2* overexpression (yellow in K′, corresponding white cells in L′) and control vector expression (yellow in K, corresponding white cells in L).

(M) Quantification of *Dlx2* rescue of neurogenesis (error bars represent SEM of quadruplicate cultures; **p < 0.01).

GFAP+ SVZ NSCs did not affect BrdU incorporation or cell viability and the expression of NSC marker *Sox2* and cell-cycle inhibitor *p16* was unaffected, suggesting that NSCs self-renewal was not impaired (Figures S4H, S4I, and S4M). After 2 days of differentiation, there were approximately 50% fewer DLX2+ cells with *Jmjd3* knockdown, and the production of Tuj1+ neurons after 4 days was reduced by nearly 5-fold (Figures 2C–2G). While *Jmjd3* knockdown did not reduce the number of GFAP+ astrocytes, the production of OLIG2+ cells and O4+ oligodendrocytes was impaired (Figures S4J–S4L). Thus, *Jmjd3* is required for proper SVZ NSC differentiation.

The *cis*-regulatory regions of *Jmjd3* harbor retinoic acid (RA) receptor response elements (Jepsen et al., 2007), and RA regulates postnatal SVZ neurogenesis in vivo (Wang et al., 2005). The addition of RA to SVZ NSCs increased *Jmjd3* expression by 2- to 3-fold, and *Dlx2* was also induced 8- to 9-fold (Figure 2H). Furthermore, transient transfection of a *Jmjd3* expression vector, but not a construct in which the catalytic JmjC domain is inactivated (*Jmjd3-Mut*) (Burgold et al., 2008), increased the expression of both *Dcx* and *Dlx2* (Figure 2I). Thus, in SVZ NSCs, *Jmjd3* can be upregulated by RA, and increased levels of *Jmjd3* induce neurogenic gene expression.

Dlx2 Overexpression Rescues Neurogenesis from *Jmjd3*-Deficient SVZ NSCs

To investigate whether *Dlx2* is a key developmental factor for *Jmjd3*-dependent neurogenesis, we enforced *Dlx2* expression in *Jmjd3*-deficient SVZ cells. GFAPp-tva SVZ cultures were first infected with LV(EnvA)-shRNA-GFP constructs. After 2 days, cultures were infected with lentiviruses that express *Dlx2* (LV-*Dlx2*-dsRed) or control (LV-AP-dsRed) (Figure 2J). Remarkably, LV-*Dlx2*-dsRed rescued neuronal differentiation from *Jmjd3*-deficient cells (Figures 2K–2M). Furthermore, injection of LV-*Dlx2*-GFP into the SVZ *hGFAP-Cre;Jmjd3*$^{F/F}$ mice increased the number of DCX+ cells (Figures S4N–S4R). Taken together, these results suggest that the activation of *Dlx2* is a key aspect of *Jmjd3*-dependent neurogenesis.

JMJD3 Is Required for Removal of H3K27me3 at Key Transcriptional Promoters in SVZ NSCs

To gain broader insight into *Jmjd3*-dependent gene expression, we performed microarray analysis. Treatment of SVZ

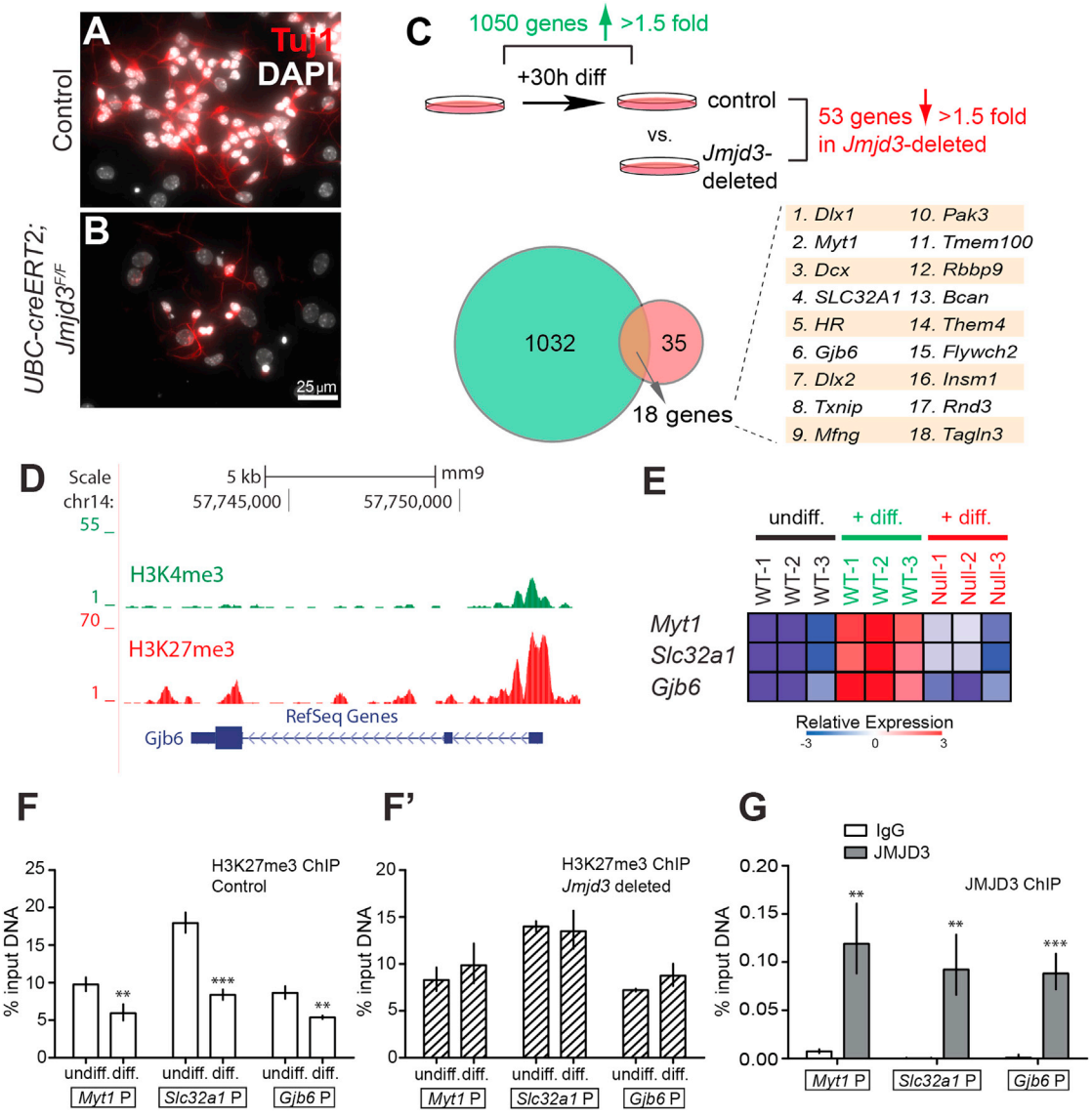

Figure 3. JMJD3 Is Required for H3K27me3 Demethylation at Neural Gene Promoters in SVZ NSCs

(A and B) ICC for Tuj1 (red) in SVZ NSC cultures from P8 *UBC-Cre/ERT2;Jmjd3*$^{F/F}$ mice after 4 days of differentiation. *Jmjd3* was deleted in SVZ NSCs by 50 nM 4-OHT treatment.

(C) Top: schematic of microarray analysis of SVZ cell differentiation and differential expression between *Jmjd3*-deleted and control cells. Bottom left: Venn diagram depicting overlap between normal gene upregulation and *Jmjd3*-dependent upregulation; 18 genes in the overlap are listed.

(D) H3K4me3 and H3K27me3 ChIP-seq enrichment tracks at the *Gjb6* locus from undifferentiated NSC cultures. H3K27me3 is enriched at the *Gjb6* promoter located at the right.

(E) Heatmap of gene expression profile for *Myt1*, *Slc32a1*, and *Gjb6*.

(F and F′) qChIP analysis of H3K27me3 in control (EtOH) and *Jmjd3*-deleted cells (4OHT) at *Myt1*, *Slc32a1*, and *Gjb6* promoters. White bars correspond to control cells. Hatched bars correspond to *Jmjd3*-deleted cells. ***p < 0.001, **p < 0.01 in comparison to proliferating cells.

(G) qChIP analysis of JMJD3 at *Myt1*, *Slc32a1*, and *Gjb6* promoters in differentiating NSCs. ***p < 0.001, **p < 0.01 compared to immunoglobulin G. Error bars represent SD; n = 3. undiff, undifferentiated SVZ NSCs; +diff, differentiated SVZ cells.

NSCs from UBC-Cre/ERT2;*Jmjd3*$^{F/F}$ mice with 4-OHT resulted in *Jmjd3* deletion, and neurogenesis was severely impaired (Figures 3A, 3B, and S5A). In nondeleted cultures, 1,050 genes were upregulated after 30 hr of differentiation (>1.5-fold; false discovery rate [FDR]-corrected p value < 0.05; n = 3). In differentiating *Jmjd3*-deleted cells, 18 of these genes, including *Dlx2*, failed to reach the same levels of expression (>1.5-fold decreased as compared to control cells; FDR-corrected p value < 0.05; n = 3; Figure 3C). Analysis of chromatin immunoprecipitation sequencing (ChIP-seq) data (Ramos et al., 2013) indicated that 12 of the 18 genes were enriched for H3K27me3 in undifferentiated SVZ NSCs (Figure 3D),

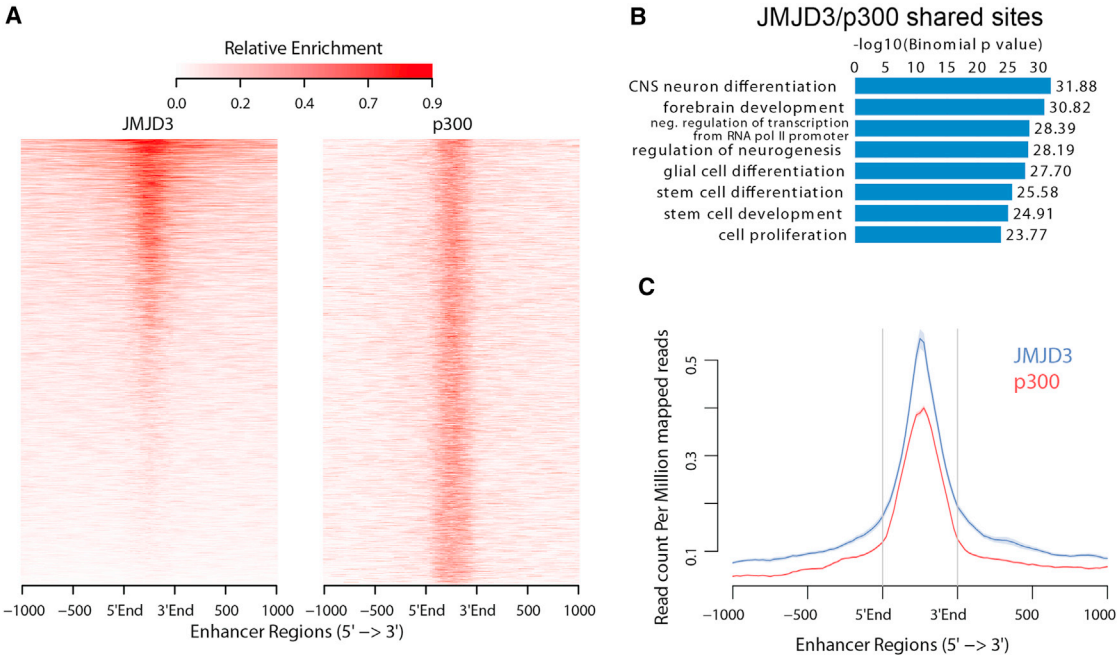

Figure 4. JMJD3 Is Enriched at Neural Transcriptional Enhancers

(A) JMJD3 and p300 enrichment across 4,425 neural enhancers and their flanking regions.

(B) The top eight enriched Gene Ontology terms identified with GREAT analysis for the 2,611 JMJD3 and p300 enriched enhancers.

(C) Averaged enrichment profile of JMJD3 and p300 across 4,425 putative neural enhancers and their flanking regions.

suggesting that removal of this repressive mark is required for their upregulation.

In differentiating SVZ cells, the increased expression of *Myt1*, *Slc32a1*, and *Gjb6*—genes involved in neurogenesis—was strongly *Jmjd3* dependent (Figure 3E). In undifferentiated NSCs, these gene promoters were enriched for H3K27me3, and in control cells, H3K27me3 levels were reduced during differentiation (Figure 3F), and JMJD3 protein was detected at these promoters (Figure 3G). In contrast, in *Jmjd3*-deleted cells, H3K27me3 levels were not decreased with differentiation (Figure 3F′). Thus, JMJD3 is required for H3K27 demethylation at specific gene promoters during SVZ NSC differentiation.

The promoter region upstream of the *Dlx2* transcriptional start site (TSS) contains regulatory elements (Ghanem et al., 2012). Interestingly, in undifferentiated SVZ NSCs, the TSS and proximal promoter was not enriched with H3K27me3 (Figure S5B). Furthermore, this low level of H3K27me3 did not change during differentiation, indicating that H3K27me3 levels at the promoter do not correlate with *Dlx2* upregulation.

JMJD3 Is Enriched at Neural Transcriptional Enhancers

Some transcriptional enhancers in stem cells exist in a poised state, which includes H3K27me3 enrichment. To investigate whether JMJD3 localizes at enhancers in neural development, we analyzed JMJD3 ChIP-seq data from NSCs derived from E12.5 mouse cortex (Estarás et al., 2012) in conjunction with p300 localization in E11.5 cortex (Visel et al., 2013). Of the 4,425 potential enhancer regions bound by p300, 2,611 (59%) exhibited JMJD3 enrichment (Figures 4A and 4C). These JMJD3-enriched enhancers correlated with brain development (McLean et al., 2010), including differentiation toward neuronal lineages (Figure 4B). Together, these data suggest that JMJD3 can regulate the chromatin state of neural-specific enhancers genome-wide. We therefore hypothesized that JMJD3 regulates *Dlx2* expression in SVZ NSCs through interactions at a key enhancer.

JMJD3 Is Required for H3K27me3 Demethylation of a *Dlx2* Enhancer

I12b is an enhancer that regulates the expression of *Dlx2* (Poitras et al., 2007) (Figure 5A). In SVZ NSC cultures, I12b had a poised chromatin state, which included high levels of H3K27me3 (Figures S5C and S5D). To analyze I12b chromatin state changes in the SVZ neurogenic lineage, we used fluorescence-activated cell sorting (FACS) to isolate GFAP+, NESTIN+ SVZ NSCs in self-renewal conditions and Tuj1+ neuroblasts 3 days after differentiation (Figures 5B–5E). In NSCs, I12b was enriched with H3K27me3. In the neuroblasts, H3K27me3 was decreased ~12-fold (Figure 5C). This reduction in H3K27me3 correlated with JMJD3 enrichment at I12b (Figure 5D). Furthermore, in neuroblasts, H3K27 acetylation (H3K27ac) was increased (Figure 5E). Thus, JMJD3 enrichment at I12b correlated with the chromatin state activation of this *Dlx2* enhancer. Another *Dlx1/2* enhancer, URE2, had lower levels of H3K27me3 that did not decrease during neuronal differentiation (Figures S5C and S5E). We therefore focused our analysis upon I12b.

We next studied SVZ NSCs with and without acute *Jmjd3* deletion. During differentiation, H3K27me3 at I12b was

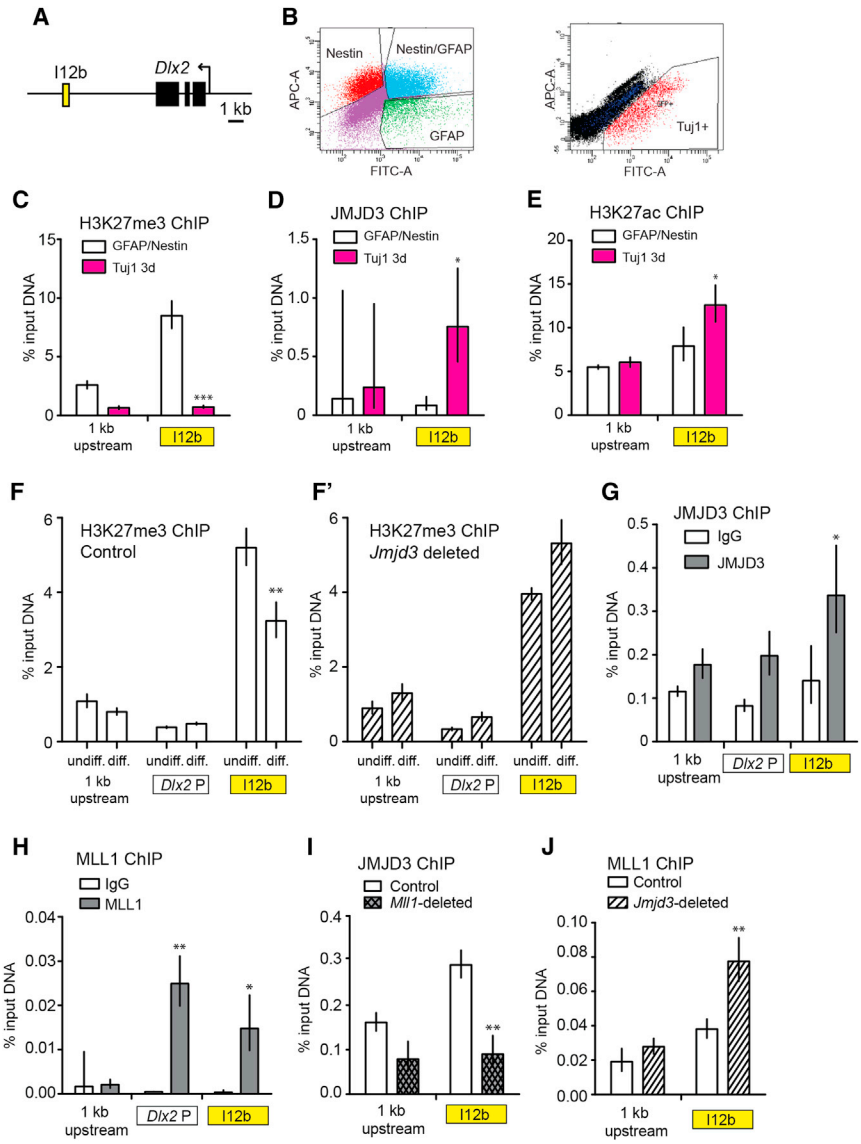

Figure 5. JMJD3 Is Required for the Activation of the I12b Enhancer

(A) The genomic region including *Dlx2* and the I12b enhancer (yellow). Arrow indicates the *Dlx2* promoter. A region 1 kb upstream of *Dlx2* was also analyzed.

(B) FACS plots of SVZ cell isolation.

(C–E) qChIP analysis of H3K27me3 (C), JMJD3 (D), and H3K27ac (E) in FACS isolated GFAP+, NESTIN+ cells and Tuj1+ cells. ***p < 0.001, *p < 0.05.

(F and F′) qChIP analysis of H3K27me3 in control (EtOH) and *Jmjd3*-deleted cells (4OHT) at the I12b enhancer and *Dlx2* promoter. White bars correspond to control cells. Hatched bars correspond to *Jmjd3*-deleted cells. **p < 0.01 compared to proliferating control cells.

(G) qChIP analysis of JMJD3 at I12b and the *Dlx2* promoter in differentiating NSCs. *p < 0.05 in comparison to 1 kb upstream region.

(H) qChIP analysis of MLL1 at *Dlx2* promoter and I12b enhancer during NSC differentiation. **p < 0.01, *p < 0.05 compared to 1 kb upstream region.

(I) qChIP analysis of JMJD3 at I12b during differentiation in control and *Mll1*-deleted cells. **p < 0.01.

(J) qChIP analysis of MLL1 at I12b during differentiation in control and *Jmjd3*-deleted cells. **p < 0.01. Error bars represent SD; n = 3. undiff, undifferentiated SVZ NSCs; +diff, differentiated SVZ cells.

DISCUSSION

Our study demonstrates that JMJD3 is required for the lifelong neurogenesis of SVZ NSCs and further illustrates mechanisms by which JMJD3 activates neurogenic gene expression. In addition to acting at gene promoters, JMJD3 also localizes to neural transcriptional enhancers and regulates the chromatin state of the I12b enhancer of *Dlx2* (Figure S5F).

decreased in control cells. In contrast, in *Jmjd3*-deleted cells, H3K27me3 did not decrease at the I12b enhancer (Figures 5F and 5F′), correlating with the lack of *Dlx2* upregulation (Figure 3C). Furthermore, JMJD3 was enriched at I12b during differentiation (Figure 5G). Thus, *Jmjd3* is required for H3K27 demethylation at the I12b enhancer.

In differentiating *Mll1*-deficient SVZ cells, the *Dlx2* locus is enriched with H3K27me3 and its transcription remains repressed (Lim et al., 2009). We therefore investigated a potential molecular-genetic relationship between *Mll1* and *Jmjd3* in the regulation of *Dlx2*. In differentiating SVZ cells, MLL1 was localized at both I12b and the *Dlx2* promoter (Figure 5H). Interestingly, in *Mll1*-deleted NSCs, JMJD3 was not enriched at I12b (Figure 5I) and *Dlx2* is not properly expressed. However, in *Jmjd3*-deleted cells, MLL1 remained enriched at I12b (Figure 5J). Taken together, these data indicate that *Mll1* is required for the enrichment of JMJD3 at I12b.

While multiple studies have indicated the critical nature of Polycomb-mediated transcriptional repression in neural development (Hirabayashi and Gotoh, 2010; Hwang et al., 2014), the role of active H3K27me3 demethylation has been less clear. How do H3K27me3-repressed genes normally become activated? While loss of H3K27me3 at specific loci could potentially be passive (e.g., through decreased EZH2 activity), EZH2 expression is not downregulated during SVZ neurogenesis (Hwang et al., 2014). In this study, we show that active H3K27me3 demethylation via JMJD3 is required for efficient expression of lineage-specific genes.

Without *Jmjd3*, SVZ NSCs appear to be "stalled" in a precursor cell state. *Jmjd3*-deficient SVZ NSCs did not efficiently activate *Dlx2* expression and were defective for neurogenesis. However, *Jmjd3* did not appear to be required for NSC identity, suggesting that *Jmjd3* does not play a key role in SVZ NSC maintenance. Interestingly, adult *hGFAP-Cre;Jmjd3*$^{F/F}$ mice had

greater numbers of cells with type B1 cell characteristics. Given that we did not observe increased cell proliferation with *Jmjd3* deficiency, it is possible that the accumulation of type B1-like cells in *hGFAP-Cre;Jmjd3*$^{F/F}$ mice relates to an increase in the proportion of symmetric, self-renewing divisions, as compared to asymmetric NSC divisions that lead to the generation of differentiated cell types.

In the developing neocortex (Estarás et al., 2012; Visel et al., 2013), we found that 59% of the mapped enhancers exhibited JMJD3 enrichment. Notably, these enhancers corresponded strongly to neuron differentiation, forebrain development, regulation of neurogenesis, and other activities consistent with NSC differentiation and cortical development. These data support a role for JMJD3 at neural enhancers genome-wide in neural precursor cells, including those in the developing brain.

The requirement of JMJD3 for H3K27me3 demethylation at the I12b enhancer does not diminish the function of JMJD3 at gene promoter regions. Indeed, JMJD3 enrichment has been mapped to 7,170 promoter regions in NSCs cultured from E12.5 cortex (Estarás et al., 2012), and JMJD3-dependent H3K27me3 demethylation occurs at a number of different neural gene promoters (Akizu et al., 2010; Burgold et al., 2008; Iida et al., 2014). In this study, we found that the promoter regions of *Myt1*, *Slc32a1*, and *Gjb6* required JMJD3 for H3K27me3 demethylation and transcriptional activation. Taken together, these data suggest that JMJD3 acts at both promoters and enhancers in NSC populations.

Although UTX (KDM6A)—the other known H3K27me3-specific demethylase (Lan et al., 2007)—is required to activate gene expression in the developing heart, *Utx* null ESCs can efficiently differentiate into neurons, suggesting that UTX is not necessary for neuronal differentiation per se (Lee et al., 2012). In SVZ NSCs, *Jmjd3* deficiency did not affect the expression of *Utx,* indicating that *Utx* alone is not sufficient to activate *Dlx2* expression, and RNAi knockdown of *Utx* in SVZ cells did not inhibit neurogenesis (data not shown). Thus, different developmental lineages may utilize UTX and JMJD3 in a nonredundant manner.

How JMJD3 becomes localized at specific genomic regions is not well known, but emerging evidence indicates that transcription factors such as SMAD3 and HES1 are involved (Dai et al., 2010; Estarás et al., 2012). JMJD3 has also been found in trithorax group (trxG) chromatin remodeling complexes (De Santa et al., 2007), and trxG family member *Mll1* is required for SVZ neurogenesis (Lim et al., 2009). In SVZ cells, we found both MLL1 and JMJD3 proteins localized at I12b, and JMJD3 enrichment at this enhancer was lost in *Mll1*-deleted cells. While these data indicate that JMJD3 requires MLL1 for localization to a key neurogenic enhancer, it remains to be determined whether MLL1 and JMJD3 physically interact at I12b. Alternatively, MLL1 may be required to mediate local chromatin modifications that enable the subsequent recruitment of JMJD3 to specific genomic regions. The discovery of this genetic interaction may provide insights into how mutations in MLL genes and H3K27me3-specific demethylases contribute to the transcriptional dysregulation of medulloblastomas (Jones et al., 2012; Parsons et al., 2011). Finally, our studies establish JMJD3 as a central player for the activation of neurogenesis from a neural stem cell population, which may help inform methods of neuronal production for therapeutic purposes.

EXPERIMENTAL PROCEDURES

Generation of *Jmjd3* Conditional Knockout Mice and Mouse Studies

Jmjd3$^{F/F}$ mice were generated, maintained, and genotyped as described previously (Iwamori et al., 2013). BrdU (50 μg/g body weight, Sigma) or EdU (10^{-2} μmol/g body weight, Invitrogen) was injected intraperitoneally. Stereotactic SVZ injections were performed essentially as described previously (Mirzadeh et al., 2008). Briefly, for adult *Jmjd3*-deletion studies, we coinjected 100 nl of adenovirus (Ad:GFAP-Cre) and LV-GFP lentivirus. For *Dlx2* overexpression, we coinjected 100 nl of LV-*Dlx2*-GFP and LV-*AP*-DsRed into the SVZ. Stereotactic SVZ coordinates were 0.5 mm anterior, 1.3 mm lateral (relative to bregma), and 1.75 mm deep to the pia. Brains were fixed by intracardiac perfusion and sectioned on a cryostat (Leica) at 12 or 16 μm thickness. After blocking, primary antibodies were incubated at 4°C overnight. Antibody dilutions are listed in the Supplemental Experimental Procedures. Whole-mount dissection and immunostaining was performed as described elsewhere (Mirzadeh et al., 2008). From each animal, we analyzed at least three separate tissue sections, and from each section, we collected more than three nonoverlapping confocal images (Leica TCS SP5X) with 20× or 63× oil objectives for quantification (ImageJ, NIH). Experiments were performed in accordance to protocols approved by Institutional Animal Care and Use Committee at University of California, San Francisco.

Cell-Culture Studies

SVZ NSC monolayer cultures were generated and analyzed as in Lim et al. (2009). High-titer pSicoR lentiviruses were produced in human embryonic kidney 293T cells as described previously (Lewis et al., 2001). For *Jmjd3* knockdown, we derived SVZ NSCs from transgenic mice that express the tva receptor under the control of the GFAP promoter (GFAPp-tva) (Holland et al., 1998). To delete *Jmjd3* in SVZ NSCs, cultures from UBC-Cre/ERT2;*Jmjd3*$^{F/F}$ mice were treated with 4-OHT (50 nM, Sigma) for 96 hr. For RA treatment and *Jmjd3* overexpression, SVZ NSC monolayer cultures were established as described previously (Brill et al., 2008). For *Jmjd3* overexpression, pCDNA-Flag *Jmjd3* and pCDNA-Flag *Jmjd3* mutant (H1388/A) (Burgold et al., 2008) were transfected using jetPRIME (Polyplus) and analyzed after 48 hr. For each culture well, we captured more than 13 nonoverlapping fields (Leica DMI4000B) with a 20× objective and analyzed them with ImageJ (NIH). Primary and secondary antibodies are listed in the Supplemental Experimental Procedures. SYTOX red (Invitrogen) was used per the manufacturer's protocol and quantified on a fluorescent flow cytometer (BD FACSAria).

ChIP, qRT-PCR, Microarray, and Bioinformatic Analysis

Quantitative ChIP (qChIP) and quantitative RT-PCR was performed essentially as previously described (Lim et al., 2009). qChIP analysis of FACS-isolated cells was performed as described previously (Hwang et al., 2014). ChIP antibodies and primer sequences and other methodological details are in the Supplemental Experimental Procedures and Table S1. For microarray analysis, biological replicates were prepared as in (Ramos et al., 2013) and hybridized to MouseRef-8 v2.0 Expression BeadChip arrays (Illumina). Array data were normalized with IlluminaNormalizer v.2 and analyzed with Cyber-T (http://cybert.ics.uci.edu/). Gene Ontology analysis was performed with DAVID. SVZ RNA-seq and SVZ NSC ChIP-seq data were analyzed as in Ramos et al. (2013). ChIP-seq data from Gene Expression Omnibus (GEO) series GSE36673, GSE42881, and GSE13845 were analyzed as follows: FASTQ reads were aligned to mm9 using Bowtie2 2.1.0 with default parameters. Tracks and peaks were generated using MACS 1.4 with default parameters. Co-occupancy analysis was performed using BEDTools against published peaks. Genomic Regions Enrichment of Annotations Tool (GREAT) analysis was performed as described previously (McLean et al., 2010). Analysis parameters and references are in the Supplemental Experimental Procedures.

ACCESSION NUMBERS

The NCBI Gene Expression Omnibus accession number for the microarray analysis reported in this paper is GSE59888.

SUPPLEMENTAL INFORMATION

Supplemental Information includes Supplemental Experimental Procedures, five figures, and three tables and can be found with this article online at http://dx.doi.org/10.1016/j.celrep.2014.07.060.

AUTHOR CONTRIBUTIONS

D.H.P. and D.A.L. conceived of the project, designed experiments, analyzed data, and wrote the manuscript. D.H.P., S.J.H., R.D.S., S.J.L., and S.W.S. performed experiments and analyzed data. J.S. and G.T. performed preliminary ChIP experiments and contributed JMJD3 antibodies. M.M.M. and N.I. contributed transgenic mice. All authors helped write and edit the manuscript.

ACKNOWLEDGMENTS

This project was supported by VA 1I01 BX000252-01, NIH DP2-OD006505-01, and the Sontag Foundation (to D.A.L.) and by the Italian Ministry of Health (Ricerca Corrente and Progetto Giovani Ricercatori 2008) and Italian Association for Cancer Research (to G.T.). We thank Drs. Arturo Alvarez-Buylla and John Rubenstein for insightful comments on this work and the manuscript.

Received: March 15, 2013
Revised: July 25, 2014
Accepted: July 31, 2014
Published: August 28, 2014

REFERENCES

Agger, K., Cloos, P.A., Christensen, J., Pasini, D., Rose, S., Rappsilber, J., Issaeva, I., Canaani, E., Salcini, A.E., and Helin, K. (2007). UTX and JMJD3 are histone H3K27 demethylases involved in HOX gene regulation and development. Nature *449*, 731–734.

Akizu, N., Estarás, C., Guerrero, L., Martí, E., and Martínez-Balbás, M.A. (2010). H3K27me3 regulates BMP activity in developing spinal cord. Development *137*, 2915–2925.

Brill, M.S., Snapyan, M., Wohlfrom, H., Ninkovic, J., Jawerka, M., Mastick, G.S., Ashery-Padan, R., Saghatelyan, A., Berninger, B., and Götz, M. (2008). A dlx2- and pax6-dependent transcriptional code for periglomerular neuron specification in the adult olfactory bulb. J. Neurosci. *28*, 6439–6452.

Burgold, T., Spreafico, F., De Santa, F., Totaro, M.G., Prosperini, E., Natoli, G., and Testa, G. (2008). The histone H3 lysine 27-specific demethylase Jmjd3 is required for neural commitment. PLoS ONE *3*, e3034.

Burgold, T., Voituron, N., Caganova, M., Tripathi, P.P., Menuet, C., Tusi, B.K., Spreafico, F., Bévengut, M., Gestreau, C., Buontempo, S., et al. (2012). The H3K27 demethylase JMJD3 is required for maintenance of the embryonic respiratory neuronal network, neonatal breathing, and survival. Cell Rep *2*, 1244–1258.

Calo, E., and Wysocka, J. (2013). Modification of enhancer chromatin: what, how, and why? Mol. Cell *49*, 825–837.

Dai, J.P., Lu, J.Y., Zhang, Y., and Shen, Y.F. (2010). Jmjd3 activates Mash1 gene in RA-induced neuronal differentiation of P19 cells. J. Cell. Biochem. *110*, 1457–1463.

De Santa, F., Totaro, M.G., Prosperini, E., Notarbartolo, S., Testa, G., and Natoli, G. (2007). The histone H3 lysine-27 demethylase Jmjd3 links inflammation to inhibition of polycomb-mediated gene silencing. Cell *130*, 1083–1094.

Estarás, C., Akizu, N., García, A., Beltrán, S., de la Cruz, X., and Martínez-Balbás, M.A. (2012). Genome-wide analysis reveals that Smad3 and JMJD3 HDM co-activate the neural developmental program. Development *139*, 2681–2691.

Fuentealba, L.C., Obernier, K., and Alvarez-Buylla, A. (2012). Adult neural stem cells bridge their niche. Cell Stem Cell *10*, 698–708.

Ghanem, N., Andrusiak, M.G., Svoboda, D., Al Lafi, S.M., Julian, L.M., McClellan, K.A., De Repentigny, Y., Kothary, R., Ekker, M., Blais, A., et al. (2012). The Rb/E2F pathway modulates neurogenesis through direct regulation of the Dlx1/Dlx2 bigene cluster. J. Neurosci. *32*, 8219–8230.

Gonzales-Roybal, G., and Lim, D.A. (2013). Chromatin-based epigenetics of adult subventricular zone neural stem cells. Front Genet *4*, 194.

Hirabayashi, Y., and Gotoh, Y. (2010). Epigenetic control of neural precursor cell fate during development. Nat. Rev. Neurosci. *11*, 377–388.

Hirabayashi, Y., Suzki, N., Tsuboi, M., Endo, T.A., Toyoda, T., Shinga, J., Koseki, H., Vidal, M., and Gotoh, Y. (2009). Polycomb limits the neurogenic competence of neural precursor cells to promote astrogenic fate transition. Neuron *63*, 600–613.

Holland, E.C., Hively, W.P., DePinho, R.A., and Varmus, H.E. (1998). A constitutively active epidermal growth factor receptor cooperates with disruption of G1 cell-cycle arrest pathways to induce glioma-like lesions in mice. Genes Dev. *12*, 3675–3685.

Hwang, W.W., Salinas, R.D., Siu, J.J., Kelley, K.W., Delgado, R.N., Paredes, M.F., Alvarez-Buylla, A., Oldham, M.C., and Lim, D.A. (2014). Distinct and separable roles for EZH2 in neurogenic astroglia. Elife *3*, e02439.

Iida, A., Iwagawa, T., Kuribayashi, H., Satoh, S., Mochizuki, Y., Baba, Y., Nakauchi, H., Furukawa, T., Koseki, H., Murakami, A., and Watanabe, S. (2014). Histone demethylase Jmjd3 is required for the development of subsets of retinal bipolar cells. Proc. Natl. Acad. Sci. USA *111*, 3751–3756.

Iwamori, N., Iwamori, T., and Matzuk, M.M. (2013). H3K27 demethylase, JMJD3, regulates fragmentation of spermatogonial cysts. PLoS ONE *8*, e72689.

Jepsen, K., Solum, D., Zhou, T., McEvilly, R.J., Kim, H.J., Glass, C.K., Hermanson, O., and Rosenfeld, M.G. (2007). SMRT-mediated repression of an H3K27 demethylase in progression from neural stem cell to neuron. Nature *450*, 415–419.

Jones, D.T., Jäger, N., Kool, M., Zichner, T., Hutter, B., Sultan, M., Cho, Y.J., Pugh, T.J., Hovestadt, V., Stütz, A.M., et al. (2012). Dissecting the genomic complexity underlying medulloblastoma. Nature *488*, 100–105.

Lan, F., Bayliss, P.E., Rinn, J.L., Whetstine, J.R., Wang, J.K., Chen, S., Iwase, S., Alpatov, R., Issaeva, I., Canaani, E., et al. (2007). A histone H3 lysine 27 demethylase regulates animal posterior development. Nature *449*, 689–694.

Lee, S., Lee, J.W., and Lee, S.K. (2012). UTX, a histone H3-lysine 27 demethylase, acts as a critical switch to activate the cardiac developmental program. Dev. Cell *22*, 25–37.

Lein, E.S., Hawrylycz, M.J., Ao, N., Ayres, M., Bensinger, A., Bernard, A., Boe, A.F., Boguski, M.S., Brockway, K.S., Byrnes, E.J., et al. (2007). Genome-wide atlas of gene expression in the adult mouse brain. Nature *445*, 168–176.

Lewis, B.C., Chinnasamy, N., Morgan, R.A., and Varmus, H.E. (2001). Development of an avian leukosis-sarcoma virus subgroup A pseudotyped lentiviral vector. J. Virol. *75*, 9339–9344.

Lim, D.A., Huang, Y.C., Swigut, T., Mirick, A.L., Garcia-Verdugo, J.M., Wysocka, J., Ernst, P., and Alvarez-Buylla, A. (2009). Chromatin remodelling factor Mll1 is essential for neurogenesis from postnatal neural stem cells. Nature *458*, 529–533.

Ma, D.K., Marchetto, M.C., Guo, J.U., Ming, G.L., Gage, F.H., and Song, H. (2010). Epigenetic choreographers of neurogenesis in the adult mammalian brain. Nat. Neurosci. *13*, 1338–1344.

Margueron, R., and Reinberg, D. (2011). The Polycomb complex PRC2 and its mark in life. Nature *469*, 343–349.

McLean, C.Y., Bristor, D., Hiller, M., Clarke, S.L., Schaar, B.T., Lowe, C.B., Wenger, A.M., and Bejerano, G. (2010). GREAT improves functional interpretation ofcis-regulatory regions. Nat. Biotechnol. *28*, 495–501.

Ming, G.L., and Song, H. (2011). Adult neurogenesis in the mammalian brain: significant answers and significant questions. Neuron *70*, 687–702.

Mirzadeh, Z., Merkle, F.T., Soriano-Navarro, M., Garcia-Verdugo, J.M., and Alvarez-Buylla, A. (2008). Neural stem cells confer unique pinwheel architecture to the ventricular surface in neurogenic regions of the adult brain. Cell Stem Cell *3*, 265–278.

Parsons, D.W., Li, M., Zhang, X., Jones, S., Leary, R.J., Lin, J.C., Boca, S.M., Carter, H., Samayoa, J., Bettegowda, C., et al. (2011). The genetic landscape of the childhood cancer medulloblastoma. Science *331*, 435–439.

Pereira, J.D., Sansom, S.N., Smith, J., Dobenecker, M.W., Tarakhovsky, A., and Livesey, F.J. (2010). Ezh2, the histone methyltransferase of PRC2, regulates the balance between self-renewal and differentiation in the cerebral cortex. Proc. Natl. Acad. Sci. USA *107*, 15957–15962.

Poitras, L., Ghanem, N., Hatch, G., and Ekker, M. (2007). The proneural determinant MASH1 regulates forebrain Dlx1/2 expression through the I12b intergenic enhancer. Development *134*, 1755–1765.

Rada-Iglesias, A., Bajpai, R., Swigut, T., Brugmann, S.A., Flynn, R.A., and Wysocka, J. (2011). A unique chromatin signature uncovers early developmental enhancers in humans. Nature *470*, 279–283.

Ramos, A.D., Diaz, A., Nellore, A., Delgado, R.N., Park, K.Y., Gonzales-Roybal, G., Oldham, M.C., Song, J.S., and Lim, D.A. (2013). Integration of genome-wide approaches identifies lncRNAs of adult neural stem cells and their progeny in vivo. Cell Stem Cell *12*, 616–628.

Satoh, T., Takeuchi, O., Vandenbon, A., Yasuda, K., Tanaka, Y., Kumagai, Y., Miyake, T., Matsushita, K., Okazaki, T., Saitoh, T., et al. (2010). The Jmjd3-Irf4 axis regulates M2 macrophage polarization and host responses against helminth infection. Nat. Immunol. *11*, 936–944.

Visel, A., Taher, L., Girgis, H., May, D., Golonzhka, O., Hoch, R.V., McKinsey, G.L., Pattabiraman, K., Silberberg, S.N., Blow, M.J., et al. (2013). A high-resolution enhancer atlas of the developing telencephalon. Cell *152*, 895–908.

Wang, T.W., Zhang, H., and Parent, J.M. (2005). Retinoic acid regulates postnatal neurogenesis in the murine subventricular zone-olfactory bulb pathway. Development *132*, 2721–2732.